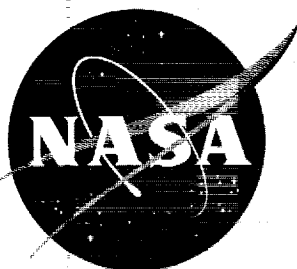


NASA TM X-30

1N-02  
380 371

NASA TM X-30



# TECHNICAL MEMORANDUM

## X-30

THE STABILIZING EFFECTIVENESS OF CONICAL FLARES  
ON BODIES WITH CONICAL NOSES

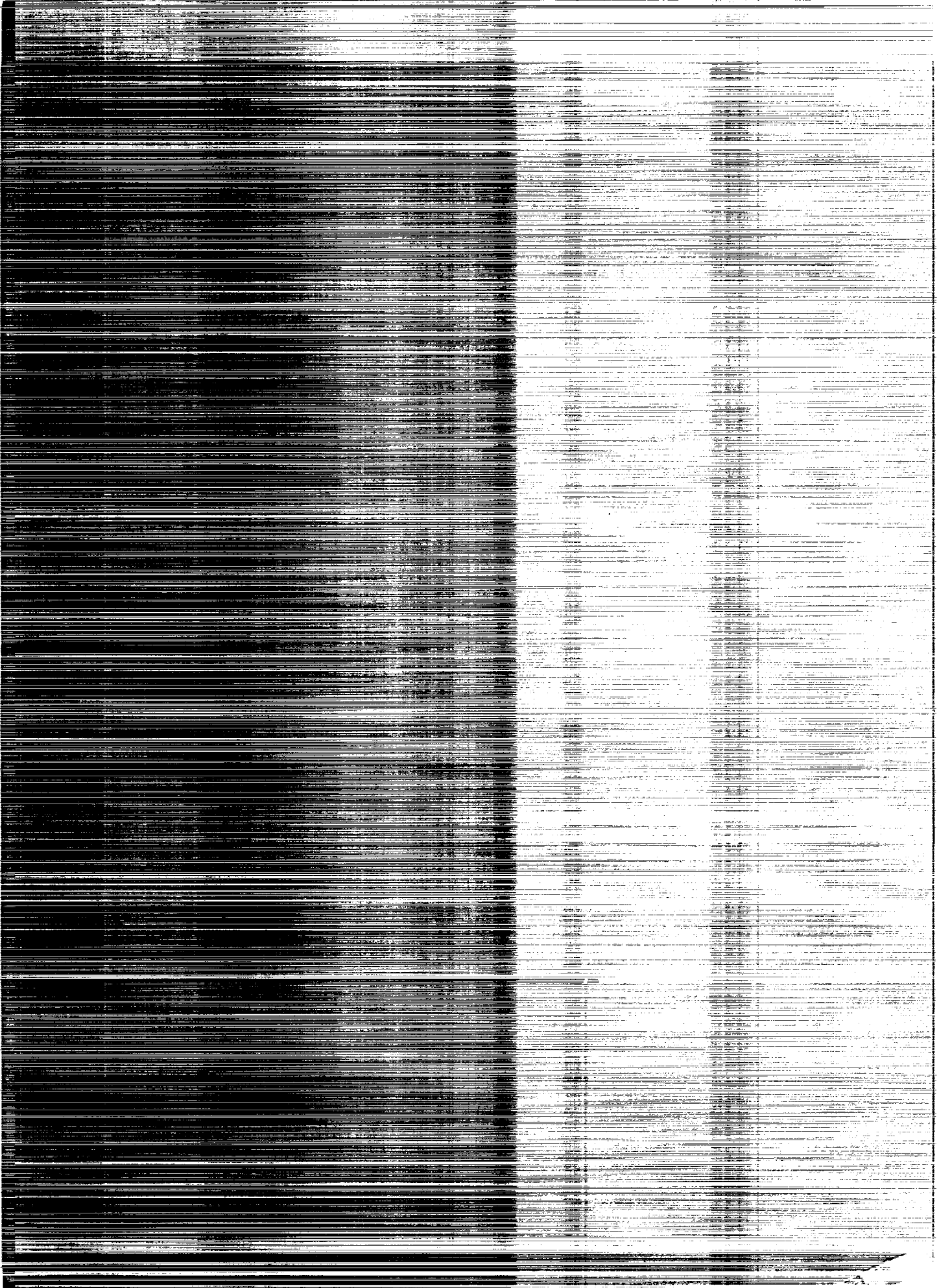
By Donn B. Kirk and Gary T. Chapman

Ames Research Center  
Moffett Field, Calif.

NATIONAL AERONAUTICS AND SPACE ADMINISTRATION  
WASHINGTON

September 1959

Declassified September 28, 1961



NATIONAL AERONAUTICS AND SPACE ADMINISTRATION

---

TECHNICAL MEMORANDUM X-30

---

THE STABILIZING EFFECTIVENESS OF CONICAL FLARES

ON BODIES WITH CONICAL NOSES

By Donn B. Kirk and Gary T. Chapman

SUMMARY

An analysis is presented of published results of force tests on 80 cone-cylinder-flare configurations at Mach numbers of 2.18, 2.81, and 4.04. The contributions, excluding interference effects, of the cone-cylinder bodies to the over-all normal force derivatives have been removed by means of the second-order shock-expansion method, and the normal force derivatives at zero angle of attack due to the flares alone are shown. The results from a wide variety of configurations are correlated by plotting ratios of the normal force derivatives of the flares to the normal force derivatives of cones having the same included angle. Comparisons are made of the experimental normal force results with the normal force derivatives obtained by assuming conical flow over the flares and with those obtained by use of the second-order shock-expansion method. The comparisons show that use of the second-order shock-expansion method is generally the superior of the two, and in most cases gives values of the normal force derivatives of the flares which agree very well with the experimental results.

Centers of pressure of the flares are presented and comparisons are made with results obtained from the theories mentioned. In general, the comparisons show that the assumption of conical flow over the flares is comparable to use of the second-order shock-expansion method in determining the centers of pressure, and in many cases both methods give values which agree closely with the experimental results.

INTRODUCTION

The effectiveness of truncated conical flares to provide longitudinal and directional stability has been estimated by several methods. The truncated cone method assigns to the flare the same normal force as would be developed by the similar portion of a cone having the same half-angle

as the flare. Although it was known that this was only an approximation, the value and limitations of this procedure have not been systematically investigated. Another method of estimation that has been used is the second-order shock-expansion method of reference 1. In order to evaluate the adequacy of these methods, experimental information was needed. This need was fulfilled in part by the large amount of data on cone-cylinder-flare configurations compiled by Redstone Arsenal (refs. 2, 3, and 4).

The purpose of this report is to compare the experimentally determined normal force derivatives and centers of pressure of the flares with those predicted by the truncated cone method and the second-order shock-expansion method. The removal of the forces due to the cone-cylinder forebodies is accomplished by use of the second-order shock-expansion method. Reference 1 shows that this method gives values of the normal force derivatives and centers of pressure for cone-cylinder bodies very close to experimental values. The stability contribution of each flare alone can then be expressed in terms of its normal force derivative and its center of pressure.

Results are presented for Mach numbers of 2.18, 2.81, and 4.04, nose cone semivertex angles of  $15^\circ$ ,  $22.5^\circ$ , and  $30^\circ$ , cylinder lengths of 1, 2, and 4 cylinder diameters, flare half-angles of  $5^\circ$ ,  $10^\circ$ ,  $15^\circ$ , and  $20^\circ$ , and a number of flare lengths.

#### SYMBOLS

$C_{N\alpha}$	normal force derivative at $\alpha = 0^\circ$ of cone-cylinder-flare body, referred to base area of cylinder (experimentally determined, refs. 2, 3, and 4)
$C_{N\alpha_{ccy}}$	normal force derivative at $\alpha = 0^\circ$ of cone-cylinder body, referred to base area of cylinder (calculated by second-order shock-expansion method)
$C_{N\alpha_f}$	normal force derivative at $\alpha = 0^\circ$ of flare, referred to base area of flare (calculated by use of eq. (1))
$C_{N\alpha_k}$	normal force derivative at $\alpha = 0^\circ$ of a cone having a half-angle equal to that of a corresponding flare, referred to base area of flare (obtained from ref. 5)
c.p.	location of center of pressure of flare from forward shoulder of flare in percent flare length (calculated by use of eq. (3))
$d_{cy}$	diameter of cylinder

$d_f$	diameter of flare base
$l_c$	length of cone
$l_{cy}$	length of cylinder
$l_f$	length of flare
$M$	free-stream Mach number
$x_{ccy}$	distance from model nose to center of pressure of cone-cylinder body (calculated by second-order shock-expansion method)
$x_f$	distance from model nose to center of pressure of flare (calculated by use of eq. (2))
$x$	distance from model nose to center of pressure of cone-cylinder-flare body (experimentally determined, refs. 2, 3, and 4)
$\alpha$	angle of attack
$\theta_c$	semivertex angle of nose cone
$\theta_f$	half-angle of flare

#### PROCEDURE

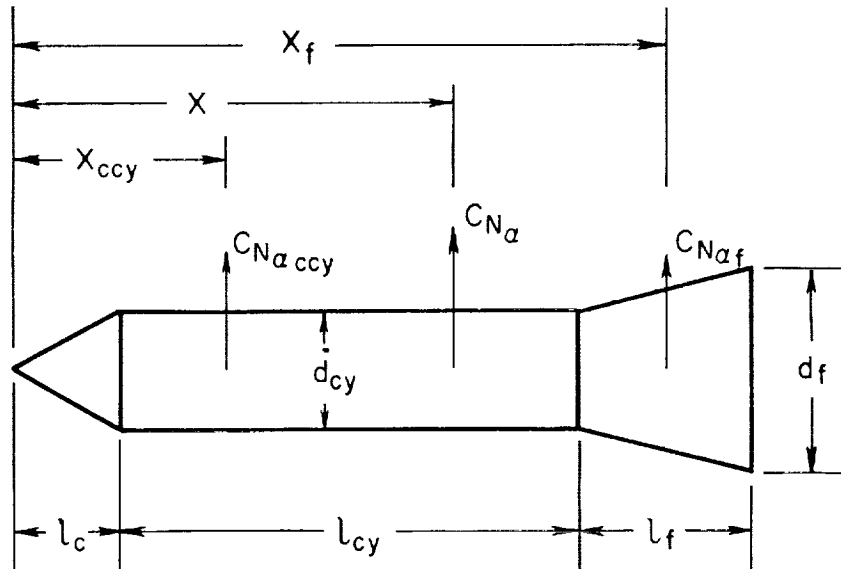
The results presented in this report were obtained by subtracting the forces due to the cone-cylinder forebodies from the experimental results in references 2, 3, and 4 by use of the second-order shock-expansion method of reference 1. This procedure is valid if the assumption is made that the flare does not alter the aerodynamic characteristics of the forebody. If there is no boundary-layer separation due to the flare, this is generally true.

In reference 1, equations are given for determining the normal force and pitching-moment derivatives of cone-cylinder bodies. The centers of pressure of the cone-cylinder bodies were obtained by dividing the pitching-moment derivatives by the corresponding normal force derivatives. The normal force derivatives and centers of pressure of the flares were obtained from the following equations (see sketch (a)).

$$C_{N\alpha_f} = \left( C_{N\alpha} - C_{N\alpha_{ccy}} \right) \left( \frac{d_{cy}}{d_f} \right)^2 \quad (1)$$

$$x_f = \frac{C_{N\alpha} x - C_{N\alpha ccy} x_{ccy}}{C_{N\alpha} - C_{N\alpha ccy}} \quad (2)$$

$$\text{c.p.} = \left( \frac{x_f - l_c - l_{cy}}{l_f} \right) 100 \quad (3)$$



Sketch (a)

The normal force derivatives were normalized to reduce the effect of the flare angle to a minimum. This was accomplished by dividing by the normal force derivative of a cone ( $C_{N\alpha_k}$ ) having the same half-angle as the flare in question. These values were obtained from reference 5.

Errors in the results presented could be introduced from two sources: experimental errors and inaccuracies of the second-order shock-expansion method in removing the forces due to the cone-cylinder forebodies. No accurate error analysis can be presented since no information on probable error was included in references 2, 3, and 4. However, several general statements regarding the accuracy of the results presented can be made by examining equations (1), (2), and (3). The flare normal force derivatives should be relatively more accurate than the flare centers of pressure since fewer factors enter into their determination. Also the effects of both sources of error on the flare normal force derivatives and centers of pressure will be most significant at the lowest diameter

ratios ( $d_f/d_{cy}$ ) and become increasingly less significant as the diameter ratio increases. The greatest variation in the flare center of pressure induced by these errors would be expected to occur when the nose cone length plus the cylinder length becomes large compared with the flare length.

## RESULTS AND DISCUSSION

Redstone Arsenal conducted tests in the California Institute of Technology Jet Propulsion Laboratory 12-inch supersonic wind tunnel of the 80 cone-cylinder-flare configurations shown in figure 1. The tests were made at Mach numbers of 2.18, 2.81, and 4.04 with approximate Reynolds number ranges based on the length from the model nose back to the compression corner of 650,000 to 2,100,000, 790,000 to 2,500,000, and 520,000 to 1,600,000, respectively. During these tests efforts were made to retain an attached boundary layer ahead of the flare. The presence of separated flow in the vicinity of the cylinder-flare junction is known to cause an increase in the normal force derivative and a rearward movement of the center of pressure on this type of body (ref. 6).

All of the models tested employed Carborundum grit on the nose cone to trip the boundary layer and thus reduce the likelihood of extensive separation. Schlieren pictures were presented in references 2, 3, and 4 showing models with and without grit. In the instances where separation was detected in these photographs, it was of a local nature, the separation point occurring very near the cylinder-flare junction. A comparison of these photographs with those presented in reference 6 which show large regions of separation emphasizes the local nature. In addition the results presented in references 2, 3, and 4 are free of any abrupt changes such as might occur in the event of a sudden change from attached flow to extensive detached flow. The experimental results presented in this report, then, are believed to be for the case of flares with primarily attached flow, and should not be used for estimates of stability when extensive regions of separated flow might be present.

The normal force data for the various cone-cylinder-flare configurations presented in references 2, 3, and 4 are nonlinear when plotted against the angle of attack, which is common for bodies of revolution. The data are most nonlinear for configurations having the longest cylinder and smallest flare angle. For the most nonlinear case, the data show a 7-percent deviation from a straight line at an angle of attack of  $4^\circ$ ; the average deviation at this angle of attack is about 2-1/2 percent. It is thus felt that the normal force derivatives at  $\alpha = 0^\circ$  presented in this report can be applied up to angles of attack of  $4^\circ$  without introducing large error.

## Normal Force Derivatives

Comparison of experimental results with truncated cone method.-  
 Figure 2 shows the normal force derivative of each flare in relation to that of a cone of the same included angle as a function of the ratio of flare base diameter to cylinder diameter at Mach number 2.18. This method of presentation largely eliminates the flare angle as a variable, and thus has the advantage of correlating results from a wide variety of configurations. The (a), (b), and (c) portions of this figure show results for different cylinder fineness ratios. In figure 2 a curve is included which shows what is obtained if the flare is considered as a cone at free-stream flow conditions with a smaller cone removed (i.e., conical flow is assumed to exist). As a first approximation, the trend of the experimental results is predicted fairly well by this curve. However, it is noted that, except in a few cases at diameter ratios below 2, the results fall below the curve, indicating that the stabilizing effectiveness of the flare has been overestimated by the truncated cone method. This is probably due to the fact that the interference effects of the forebody on the flare are not taken into account by this method. As the diameter ratio is increased, the flare becomes the major component of the configuration and the interference produced by the relatively small forebody should become less significant. The results tend to bear this out since they appear to approach the truncated cone value at high values of the diameter ratio.

The results for the  $10^\circ$ ,  $15^\circ$ , and  $20^\circ$  flares tend to fall on a single curve. It is noted, however, that the results for the  $5^\circ$  flares (open symbols) fall on a different curve, somewhat higher than for the larger flare angles. The reason for this is thought to be associated with the two-dimensional pressures which exist on the flares immediately behind the cylinder-flare junction. Some insight into this can be obtained by comparing the change in pressure with angle of attack, as a function of the flow deflection angle, for a wedge and a cone of the same semivertex angle. In the following table, the pressure derivatives,  $C_{p_\alpha}$ , are compared at a Mach number of 2.81.

$\theta_f$ , deg	$C_{p_\alpha \text{wedge}}$	$C_{p_\alpha \text{cone}}$	$\frac{C_{p_\alpha \text{wedge}}}{C_{p_\alpha \text{cone}}}$
0	0.76	0.20	3.80
5	1.02	.51	2.00
10	1.30	.82	1.59
15	1.60	1.13	1.42
20	1.97	1.44	1.37



The table shows that larger normal force will be developed by wedges than by cones for all of the above flare angles but, at small flare angles, the advantages of two-dimensional flow in generating normal force become pronounced. Therefore it is to be expected that the normal force derivative will be largest for flares having small angles as long as the region of two-dimensional flow is significant in relation to the total area. Similar trends are found at the other Mach numbers considered in this report.

Changing the cylinder length changes the flow field approaching the flare and would be expected to modify the flare normal force derivative. This effect is shown in figure 2. The difference between the experimental results and the truncated cone values is small for the bodies having the shortest cylinders but increases with increasing cylinder length. For example, at a diameter ratio of 1.5, the flare effectiveness is reduced about 50 percent as the cylinder fineness ratio is increased from 1 to 4. Additional unpublished data obtained from tests conducted in the Ames supersonic free-flight facility of models having cylinders with fineness ratios of 10 indicate that this trend continues. The primary reason for the drop in flare effectiveness with increasing cylinder fineness ratio is probably the nonviscous interference effects of the forebody on the flare. Another reason which could account for part of this dropoff is associated with the thicker boundary layer that is developed on the longer cylinders (i.e., viscous effects).

The effect of changing the nose cone semivertex angle is shown in figures 2(a) and 2(c). It is evident that, at least between  $15^\circ$  and  $30^\circ$ , the effect is generally small.

Figures 3 and 4 present results comparable to the results of figure 2, but for Mach numbers of 2.81 and 4.04, respectively. For the most part, the trends of these results are the same as at Mach number 2.18. It is noted that at Mach number 4.04 several points at high values of the diameter ratio fall above the truncated-cone value. It is felt that separation occurred during tests of these particular configurations since bodies having the shorter cylinders and largest flare angles showed this trend. These are the bodies which show evidence of local separation in the schlieren pictures presented in reference 4.

A comparison of figures 2, 3, and 4 shows the combined effect of Mach number and Reynolds number. Since the Mach number and Reynolds number were both varied, no adequate separation of the two effects can be made, but the combined effect is seen to be small.

Comparison of experimental results with second-order shock-expansion method.- Some of the results presented in figures 2, 3, and 4 are reproduced in figures 5, 6, and 7. In these figures, comparison for several representative configurations is made with values of the normal force derivative of the flare obtained by means of the second-order shock-

expansion method of reference 1.<sup>1</sup> The curve obtained by means of the truncated cone method is included in these figures for comparison.

Figure 5 ( $M = 2.18$ ) shows excellent agreement between the experimental results and the predictions made with the second-order shock-expansion method for configurations having the shortest cylinder. The second-order shock-expansion method indicates some decrease in flare effectiveness with increasing cylinder length, but not as much as the experimental results show. This is most pronounced for configurations having the largest flare angle. Figure 6 ( $M = 2.81$ ) shows the same trends as figure 5. For configurations having the shortest cylinder, figure 7 ( $M = 4.04$ ) shows poorer agreement with the experimental results than was evidenced at the other Mach numbers. At the high diameter ratios, this is due to the separation effects discussed previously. At the low diameter ratios, it could be due to either separation effects or inadequacies in the second-order shock-expansion method in removing the forces on the cone-cylinder forebody. For configurations having the longest cylinder, agreement is better at high diameter ratios than it was at the other Mach numbers.

Thus it is noted that in most cases, the second-order shock-expansion method is superior to the truncated-cone method in predicting the flare stabilizing effectiveness. It should be noted, however, that the truncated cone method takes very little time to apply relative to the second-order shock-expansion method. The truncated cone method requires approximately 5 minutes of work, whereas the second-order shock-expansion method entails the development of the flow field over the length of the forebody and flare.

#### Centers of Pressure

Comparison of experimental results with truncated cone method.- The flare center-of-pressure results are presented in figures 8, 9, and 10. For comparison, curves are included which show the centers of pressure of flares with constant pressure over their length (i.e., assumption of conical flow).

At diameter ratios greater than 2, it is noted that the centers of pressure obtained from experimental results are relatively unaffected by nose cone angle, cylinder length, and the combined effect of Mach number and Reynolds number. In this range, the center of pressure moves aft as

---

<sup>1</sup>It should be pointed out that equations (B18) and (B21) in reference 1 are incorrect, and should be changed to agree with the errata of 4-7-58. Because of these changes, the comparisons with the second-order shock-expansion method made in references 3 and 4 are in error.

the diameter ratio increases and appears to approach the cone value at high values of the diameter ratio. At diameter ratios less than 2, large movements of the center of pressure are noted. As was mentioned previously, this is the range where the flare center of pressure would be most affected by any experimental errors or inadequacies of the second-order shock-expansion method in removing the forces due to the cone-cylinder forebody. It is thus expected that these extreme movements of the center of pressure are not realistic. It is felt, however, that for some configurations the center of pressure does move somewhat forward of the 50-percent point at low values of the diameter ratio because of the influence of the two-dimensional pressures near the cylinder-flare junction.

For all the configurations having diameter ratios greater than 2, the predictions made with the truncated cone method are fairly good. At diameter ratios less than 2, the adequacy of this method cannot be determined because of the possible errors mentioned above.

Comparison of experimental results with second-order shock-expansion method.- Some of the results presented in figures 8, 9, and 10 are reproduced in figures 11, 12, and 13. In these figures, comparison for several representative configurations is made with values of the flare center of pressure obtained by means of the second-order shock-expansion method of reference 1. In general, the second-order shock-expansion method predicts the experimental center of pressure with about the same degree of accuracy as does the truncated cone method.

## CONCLUSIONS

An analysis has been made of experimental results at Mach numbers of 2.18, 2.81, and 4.04 of truncated conical flares on bodies having conical noses with semivertex angles between  $15^{\circ}$  and  $30^{\circ}$  followed by cylindrical sections 1 to 4 cylinder diameters long. Comparison of the experimental results were made with values of the flare normal force derivatives and centers of pressure obtained by use of the truncated cone method and the second-order shock-expansion method. Conclusions from this analysis are as follows:

1. The ratio of the normal force derivative of a flare to that of a cone having the same included angle is relatively independent of the flare angle and therefore is a useful parameter for correlating results from a wide variety of configurations. This normal force parameter increases with an increase of the ratio of flare base diameter to cylinder diameter and decreases with an increase in the cylinder fineness ratio.

2. Use of the truncated cone method to predict the normal force derivatives of the flares gives values which generally overestimate the

experimental results. Use of the second-order shock-expansion method to predict the normal force derivatives of the flares gives values which agree very well with the experimental results in most cases.

3. The centers of pressure of the flares obtained from experimental results are defined with precision only at diameter ratios greater than 2. For these cases the centers of pressure are relatively independent of changes in the forebody geometry and are primarily a function of the flare angle and the ratio of flare base diameter to cylinder diameter. Increasing either the flare angle or the ratio of flare base diameter to cylinder diameter results in a rearward movement of the center of pressure.

4. At diameter ratios above 2, the centers of pressure of the flares are predicted fairly well by use of either the truncated cone method or the second-order shock-expansion method.

Ames Research Center  
National Aeronautics and Space Administration  
Moffett Field, Calif., June 9, 1959

#### REFERENCES

1. Syvertson, Clarence A., and Dennis, David H.: A Second-Order Shock-Expansion Method Applicable to Bodies of Revolution Near Zero Lift. NACA Rep. 1328, 1957.
2. Lavender, Robert E., Henderson, James H., and Deep, Raymond A.: Normal Force, Pitching Moment, and Center of Pressure of Eighty Cone-Cylinder-Frustum Bodies of Revolution at Mach Number 2.18. Redstone Arsenal Rep. 6R3P, 1956.
3. Sims, Joseph L., and Henderson, James H.: Normal Force, Pitching Moment, and Center of Pressure of Eighty Cone-Cylinder-Frustum Bodies of Revolution at Mach Number 2.81. Redstone Arsenal Rep. 6R3N2, 1956.
4. Henderson, James H., and Sims, Joseph L.: Normal Force, Pitching Moment, and Center of Pressure of Eighty Cone-Cylinder-Frustum Bodies of Revolution at Mach Number 4.04. Redstone Arsenal Rep. 6R3N1, 1956.
5. Ames Research Staff: Equations, Tables, and Charts for Compressible Flow. NACA Rep. 1135, 1953.
6. Dennis, David H.: The Effects of Boundary-Layer Separation Over Bodies of Revolution With Conical Tail Flares. NACA RM A57I30, 1957.

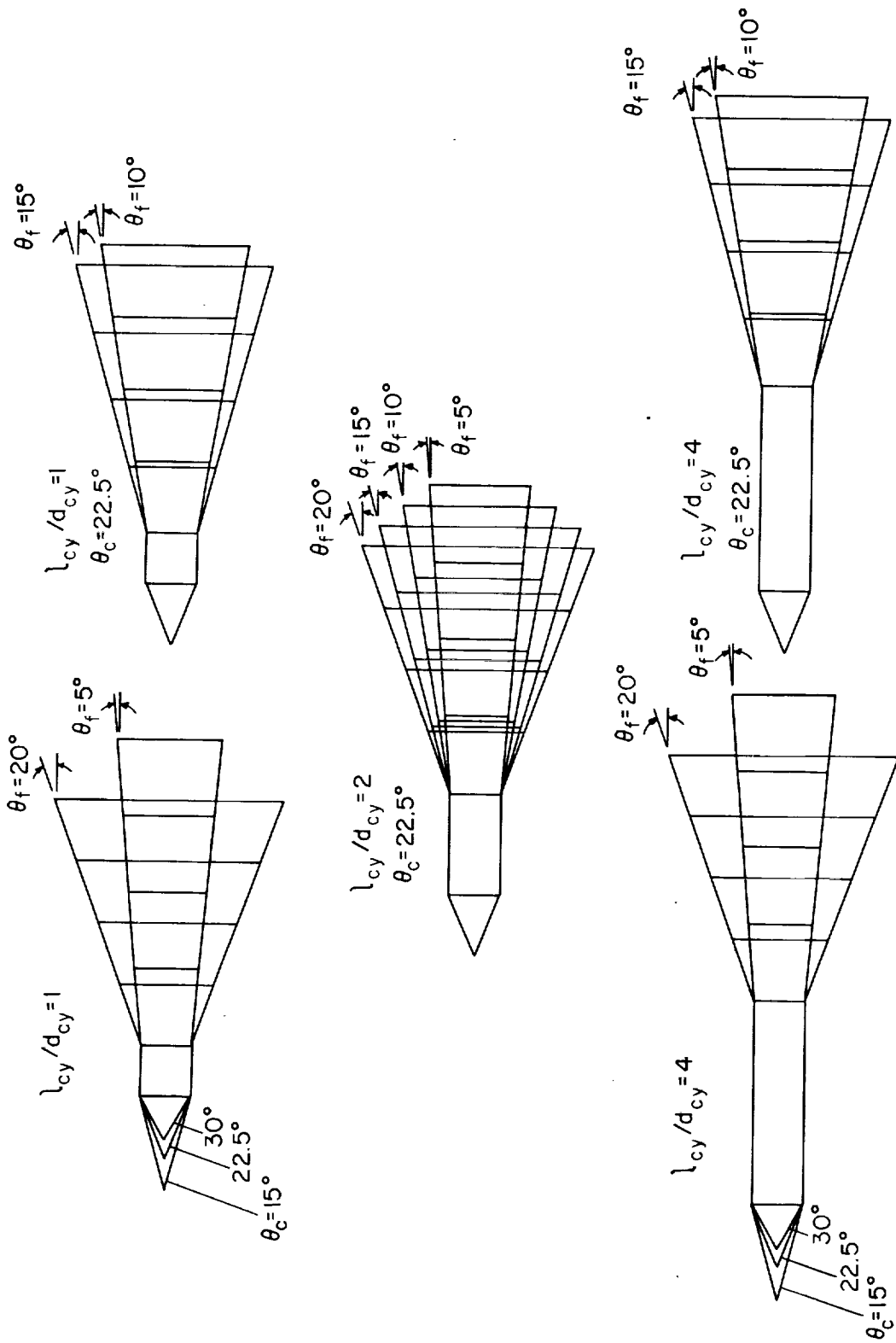


Figure 1.- Model configurations.

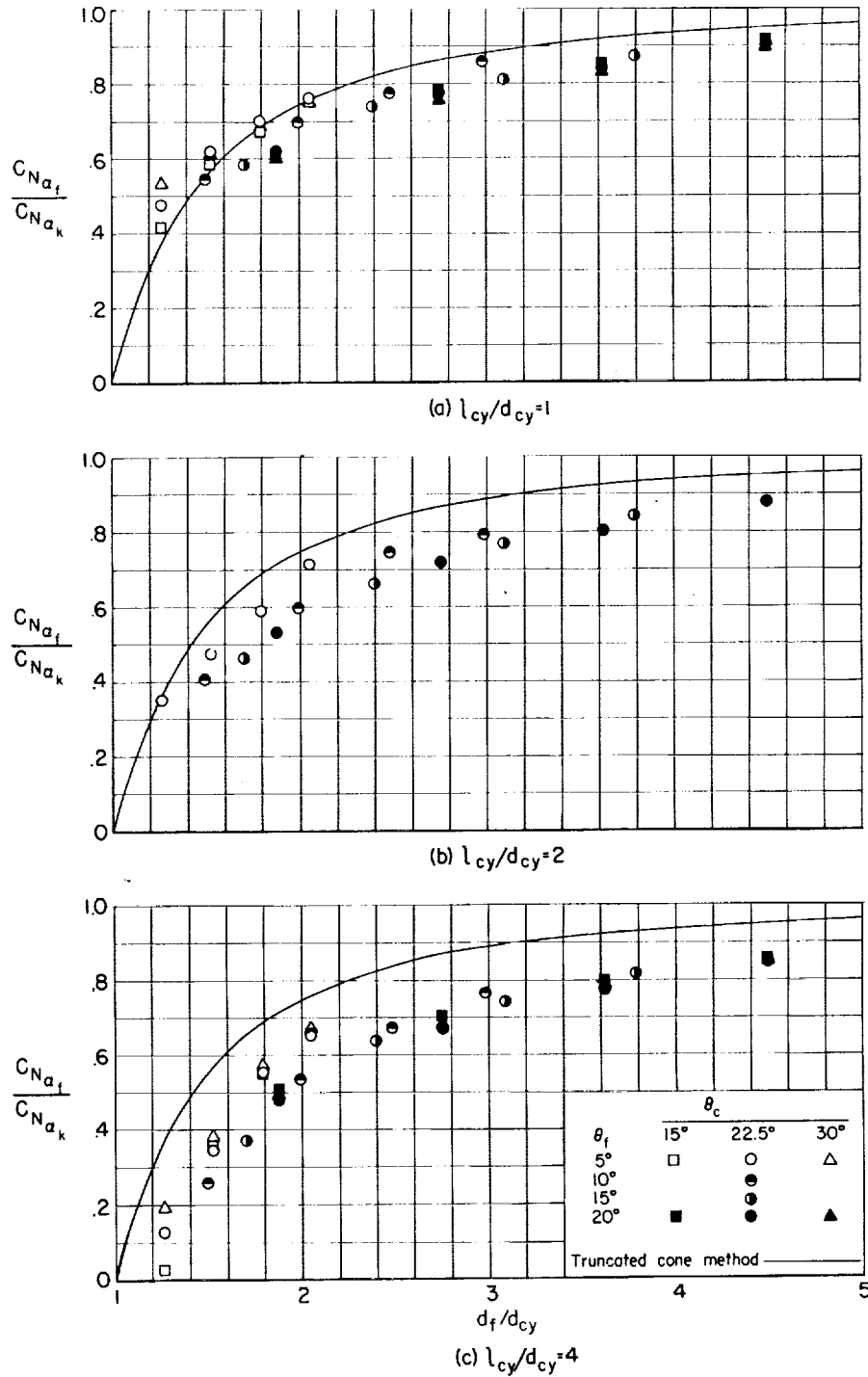


Figure 2.- Comparison of the flare normal force derivative with that predicted by use of the truncated cone method,  $M = 2.18$ .

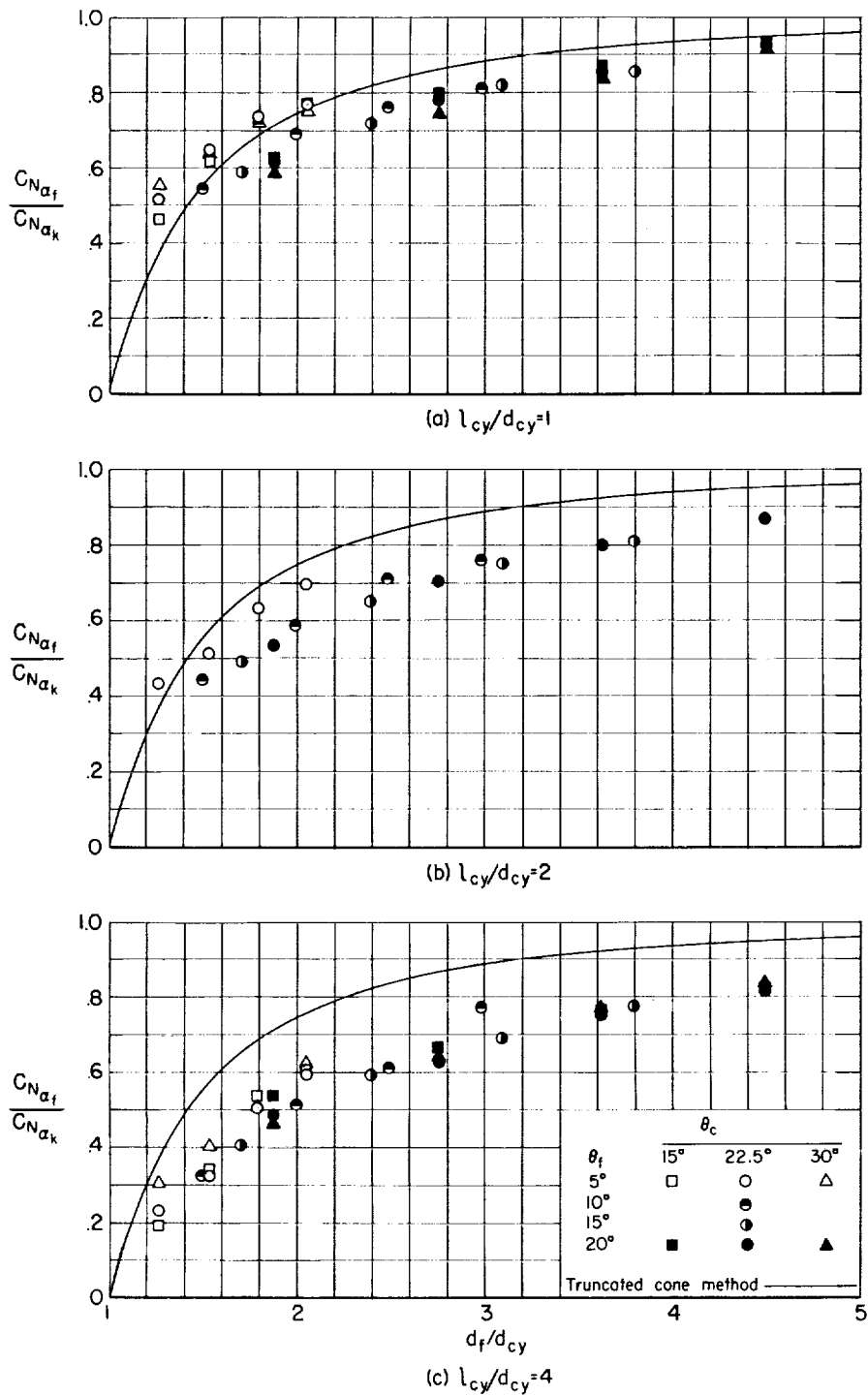


Figure 3.- Comparison of the flare normal force derivative with that predicted by use of the truncated cone method,  $M = 2.81$ .

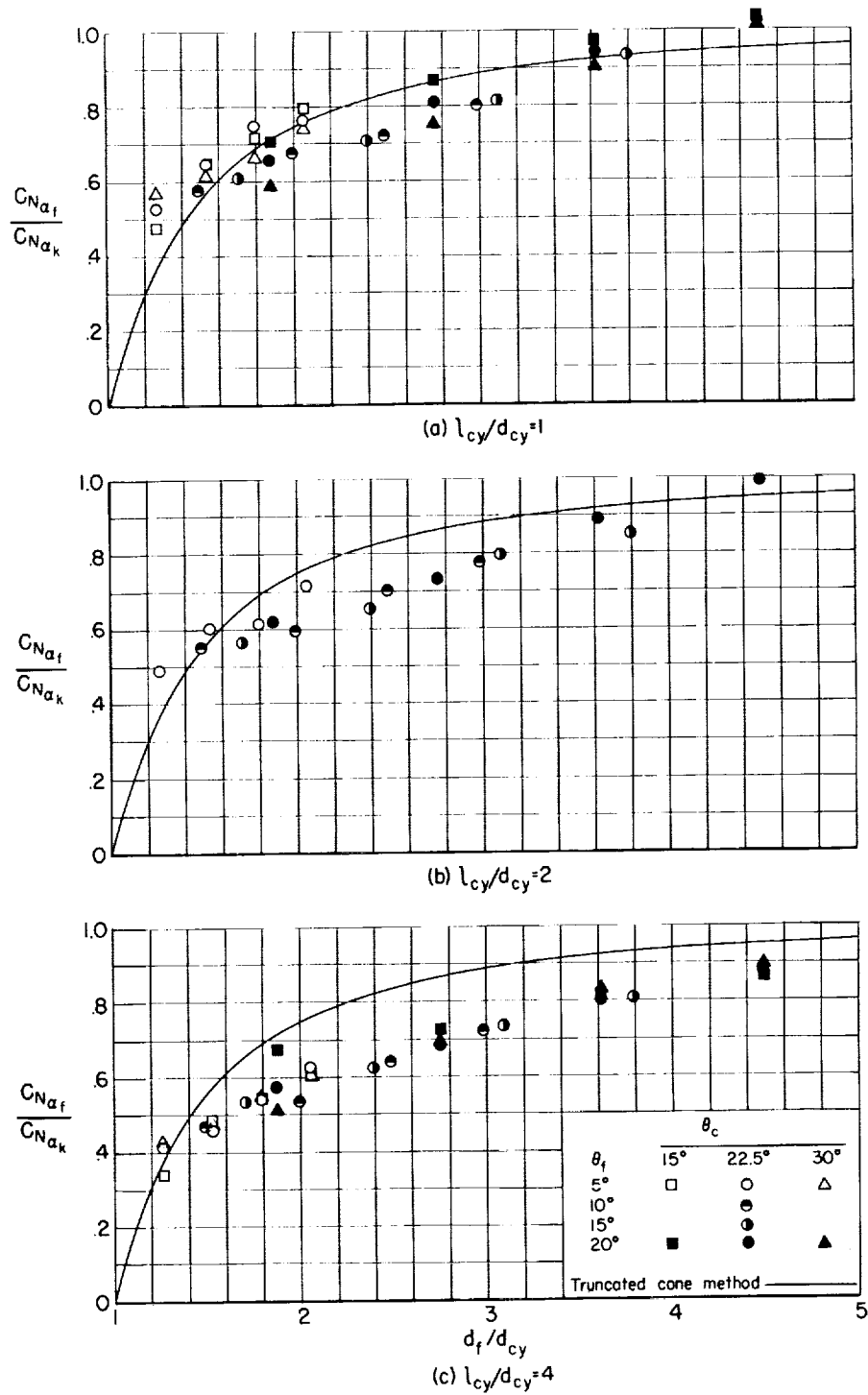


Figure 4.- Comparison of the flare normal force derivative with that predicted by use of the truncated cone method,  $M = 4.04$ .



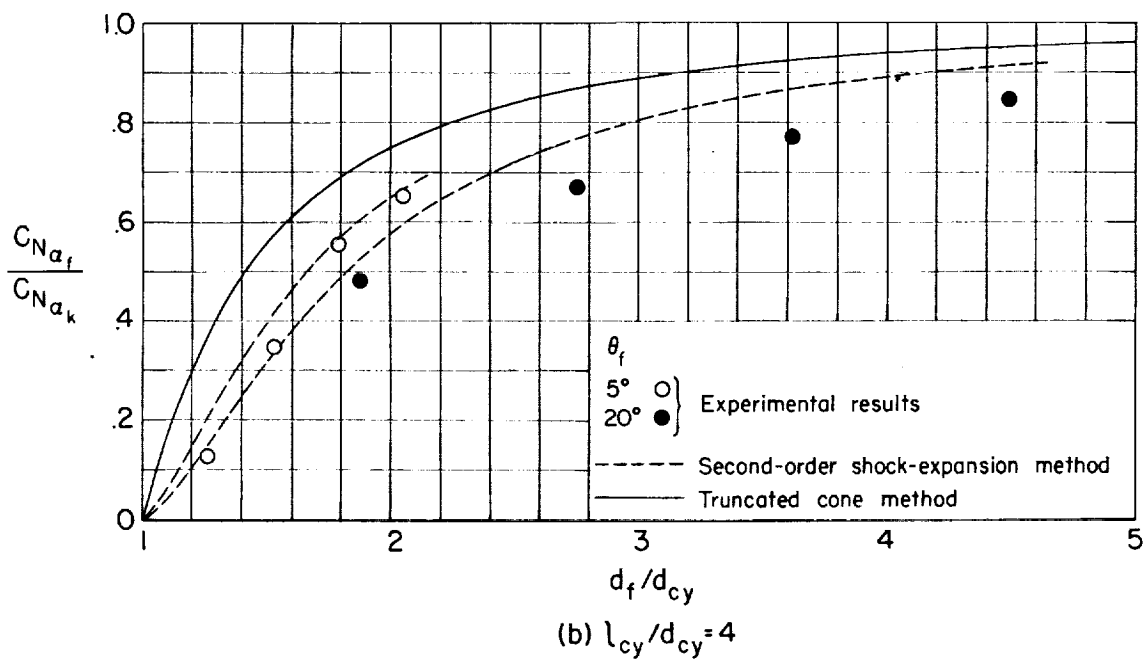
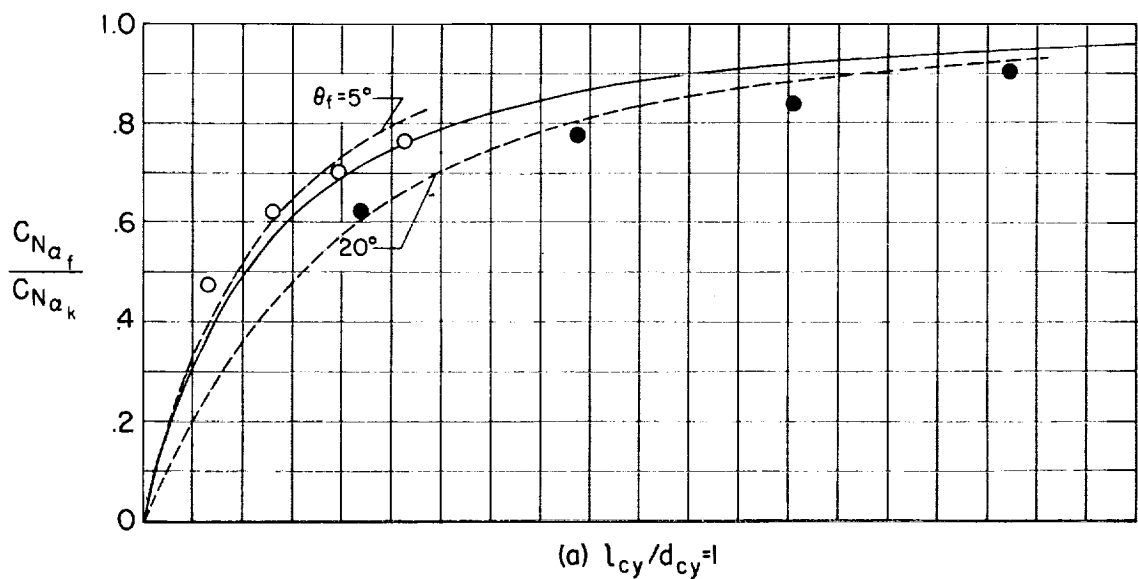


Figure 5.- Comparison of the flare normal force derivative with that predicted by use of the second-order shock-expansion method,  $M = 2.18$ .

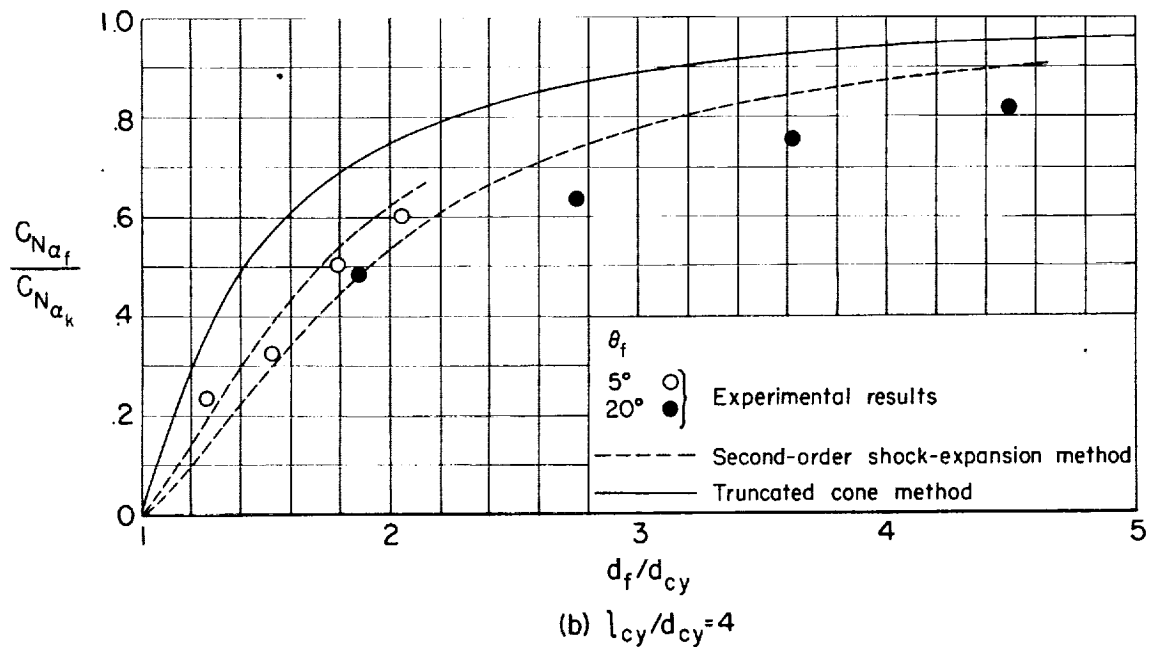
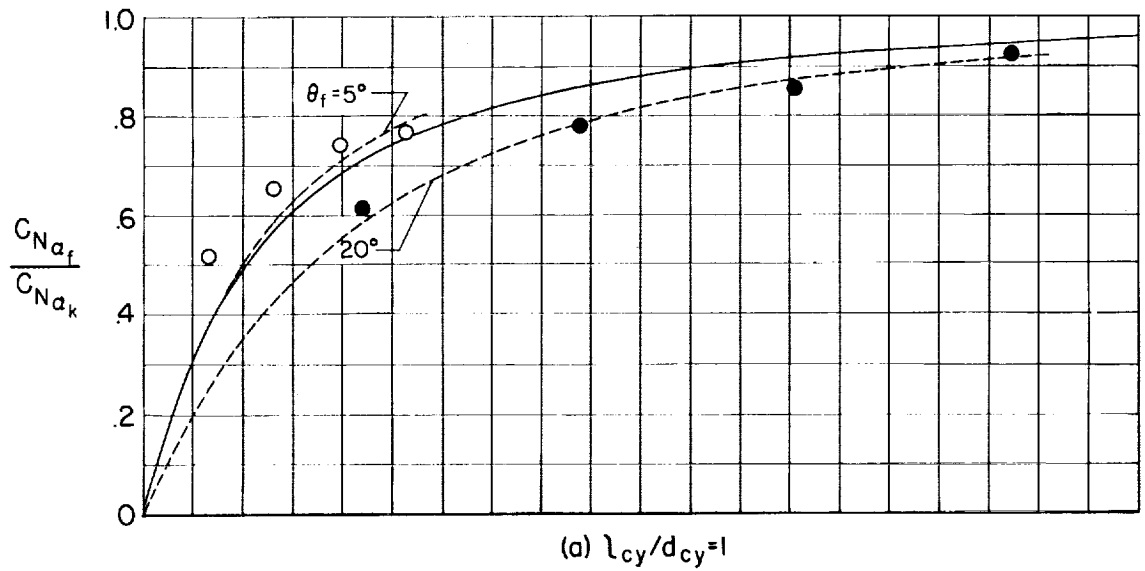


Figure 6.- Comparison of the flare normal force derivative with that predicted by use of the second-order shock-expansion method,  $M = 2.81$ .

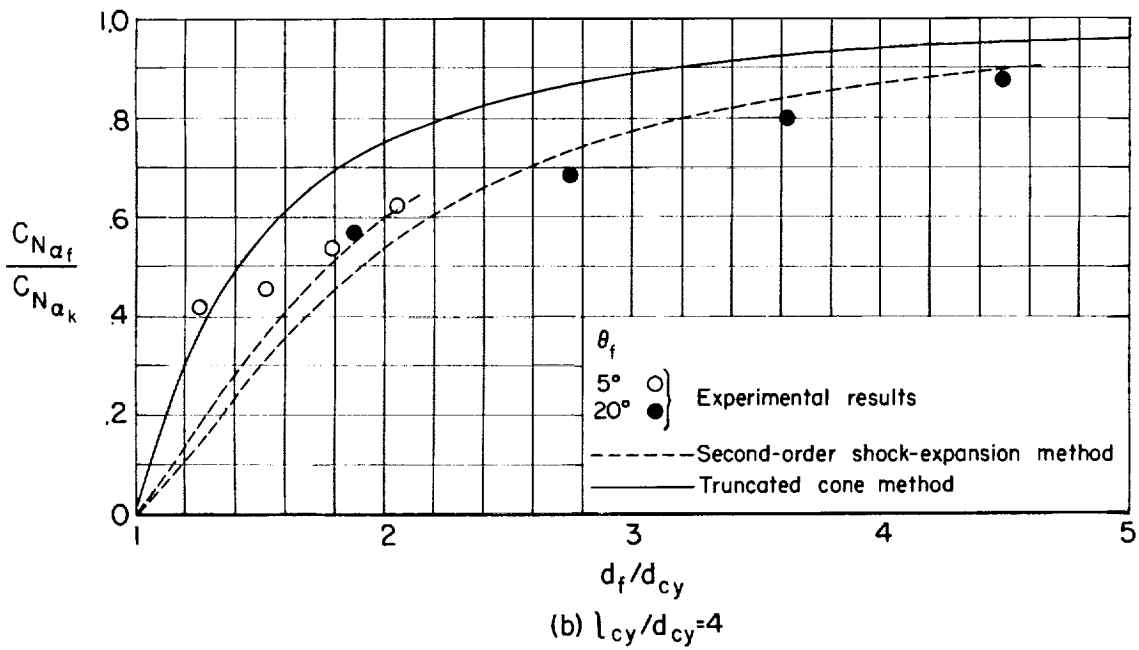
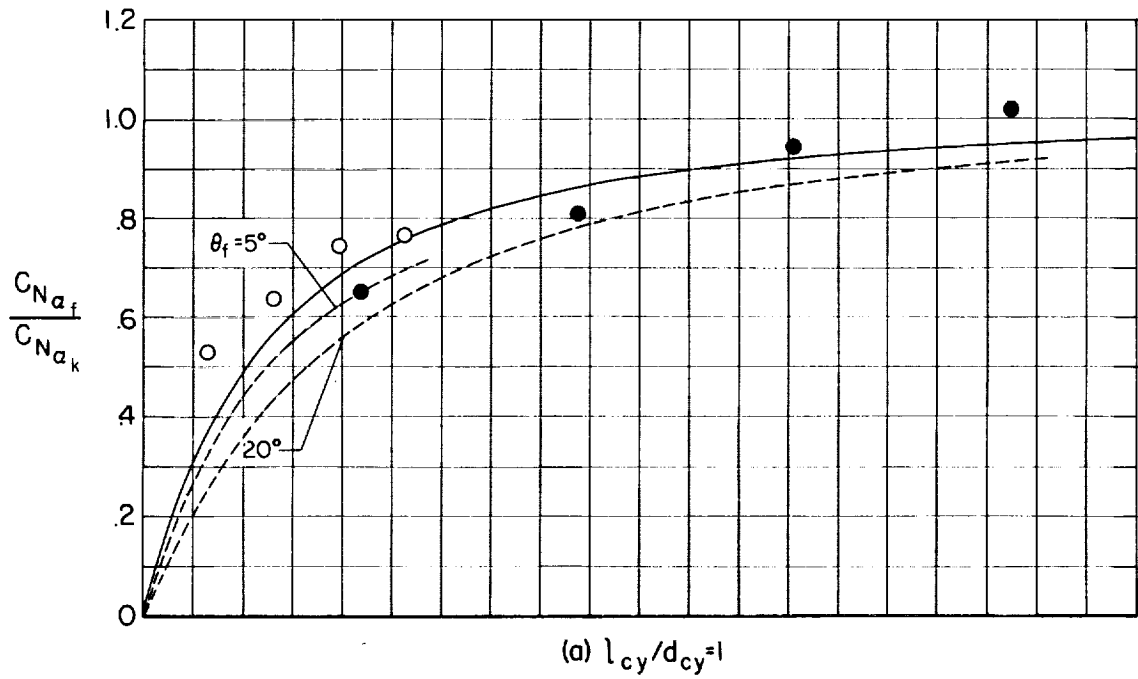


Figure 7.- Comparison of the flare normal force derivative with that predicted by use of the second-order shock-expansion method,  $M = 4.04$ .

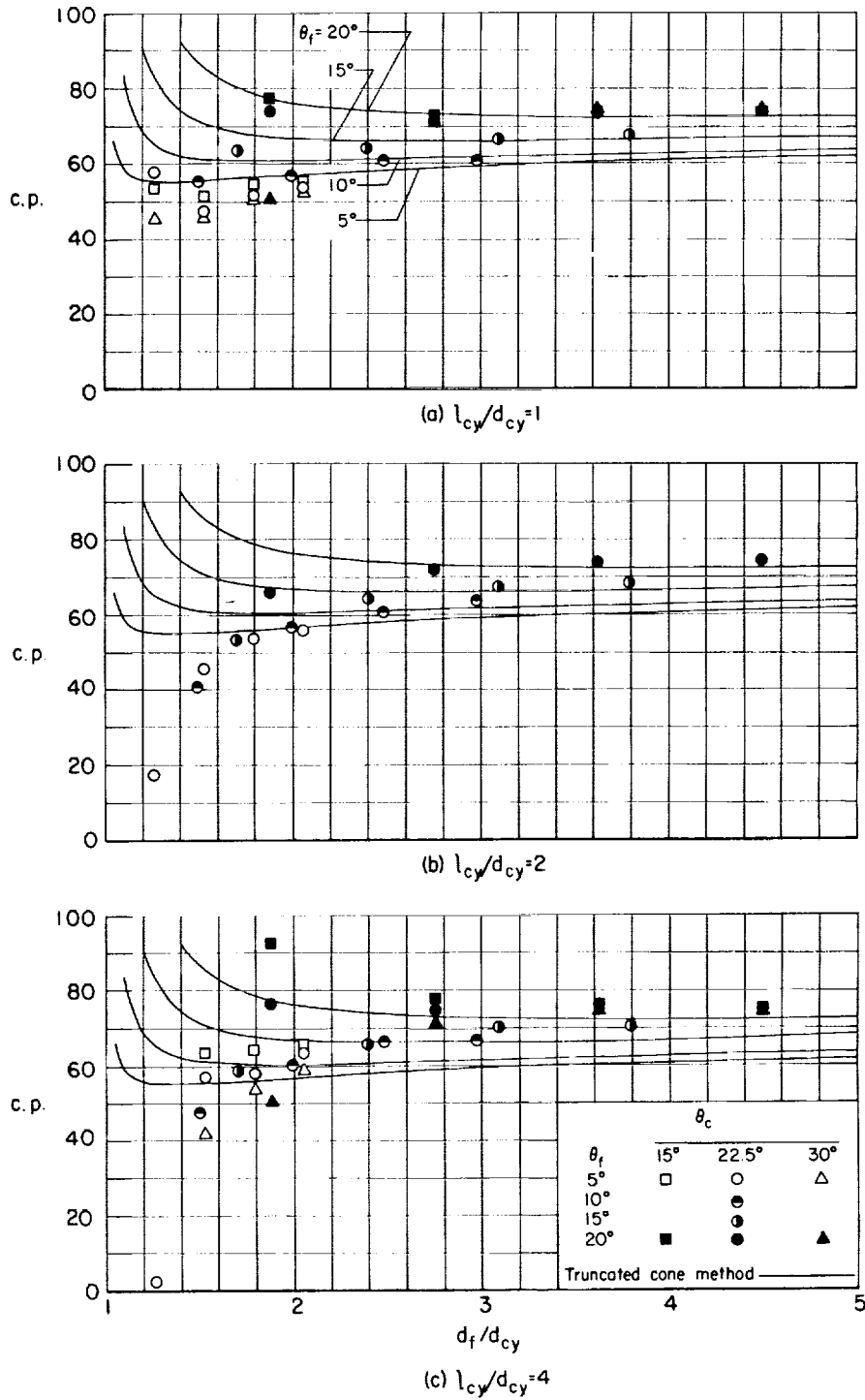


Figure 8.- Comparison of the flare center of pressure with that predicted by use of the truncated cone method,  $M = 2.18$ .

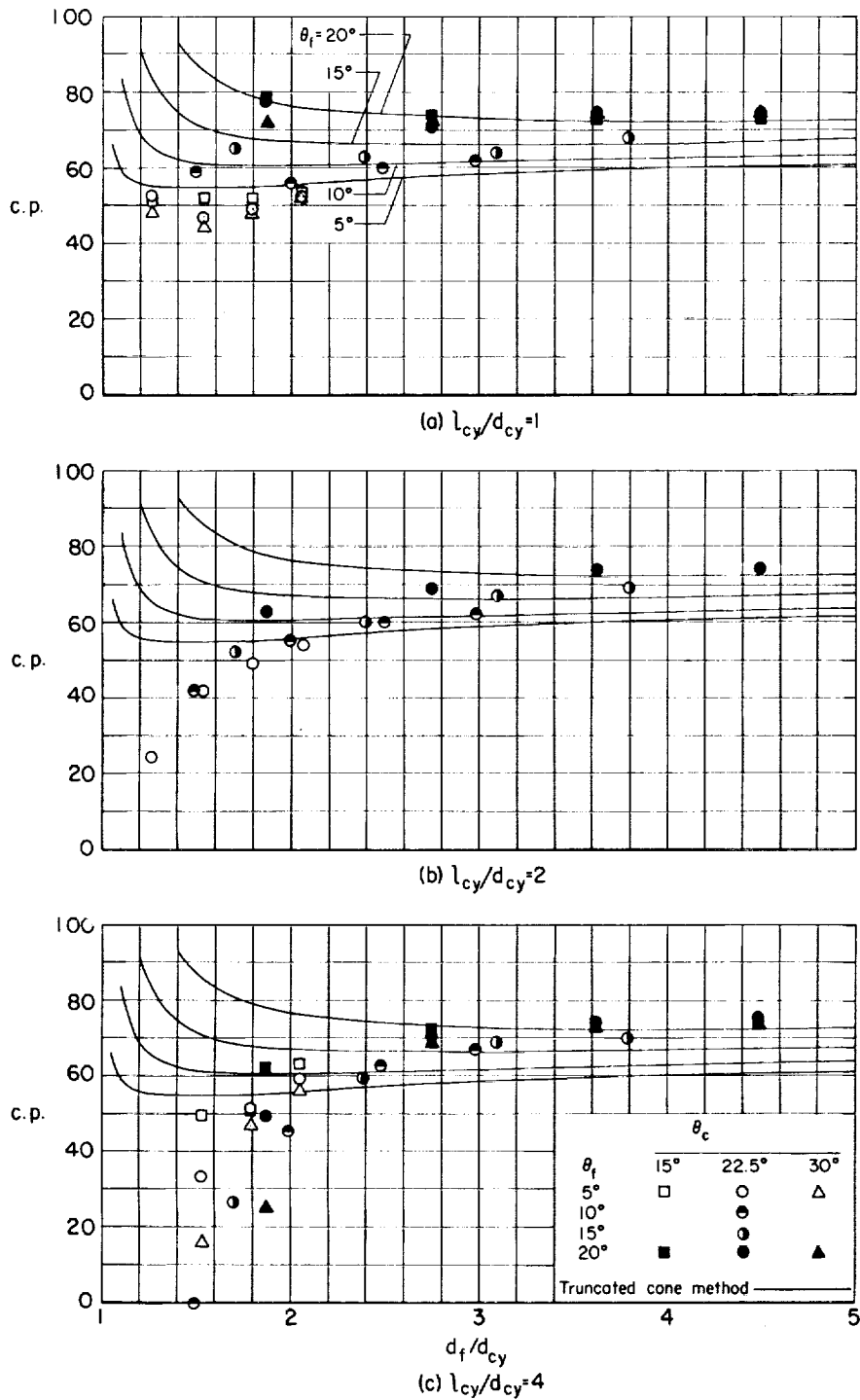


Figure 9.- Comparison of the flare center of pressure with that predicted by use of the truncated cone method,  $M = 2.81$ .

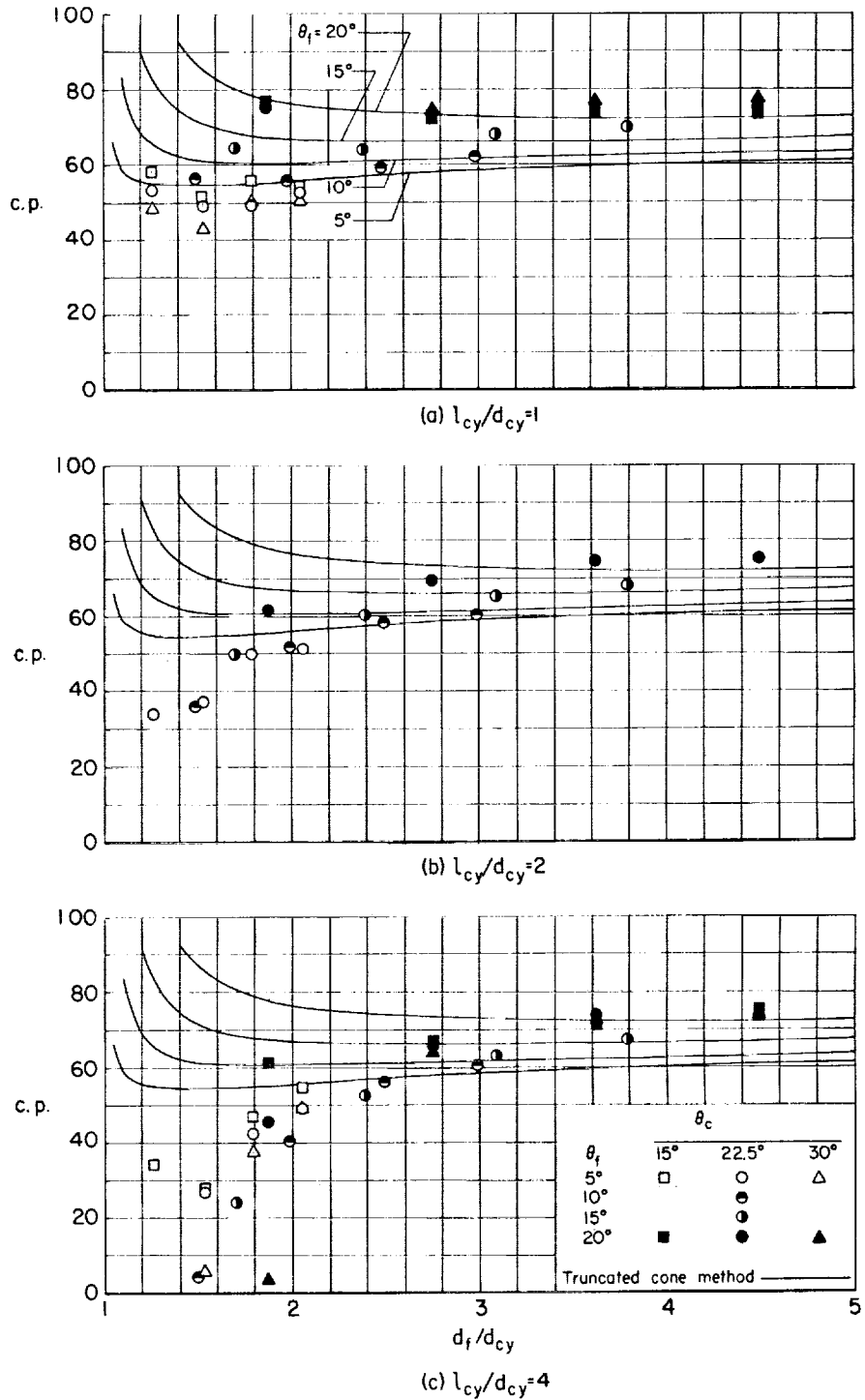


Figure 10.- Comparison of the flare center of pressure with that predicted by use of the truncated cone method,  $M = 4.04$ .

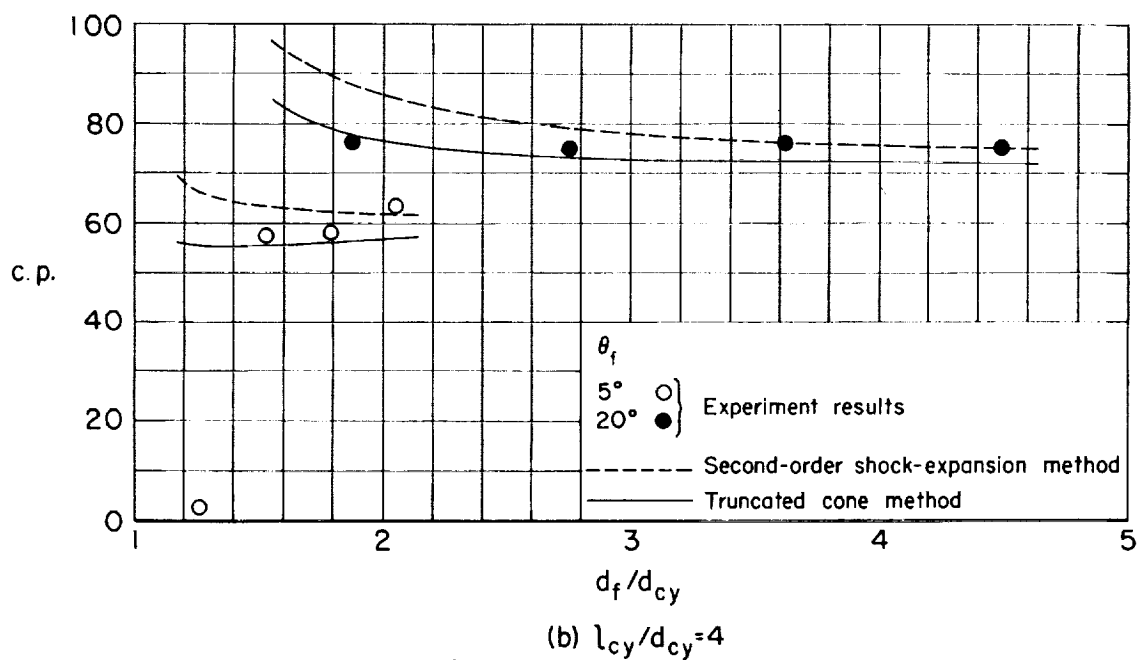
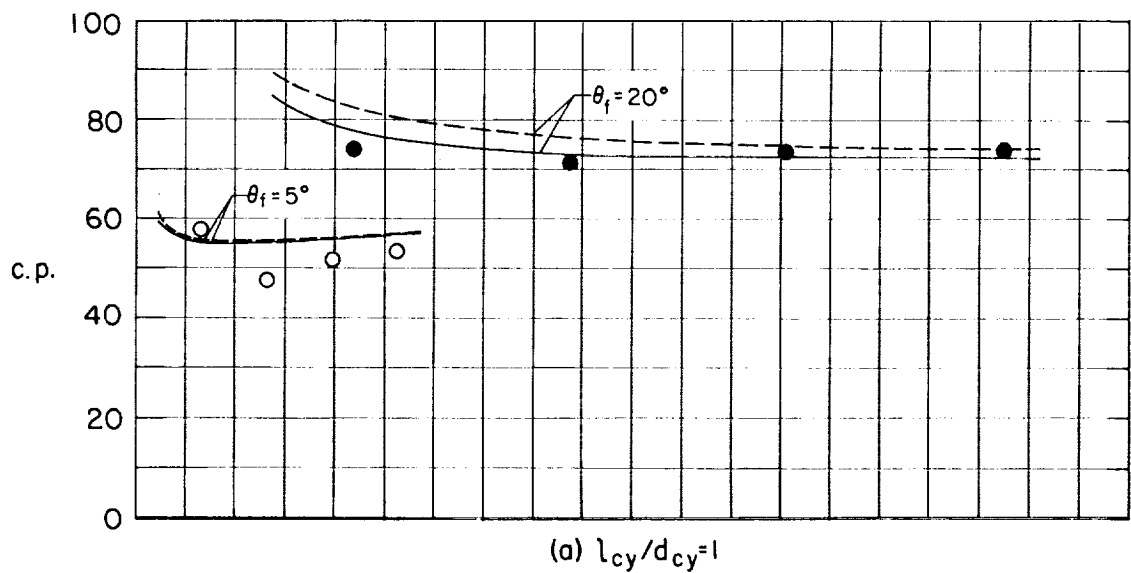


Figure 11.- Comparison of the flare center of pressure with that predicted by use of the second-order shock-expansion method,  $M = 2.18$ .

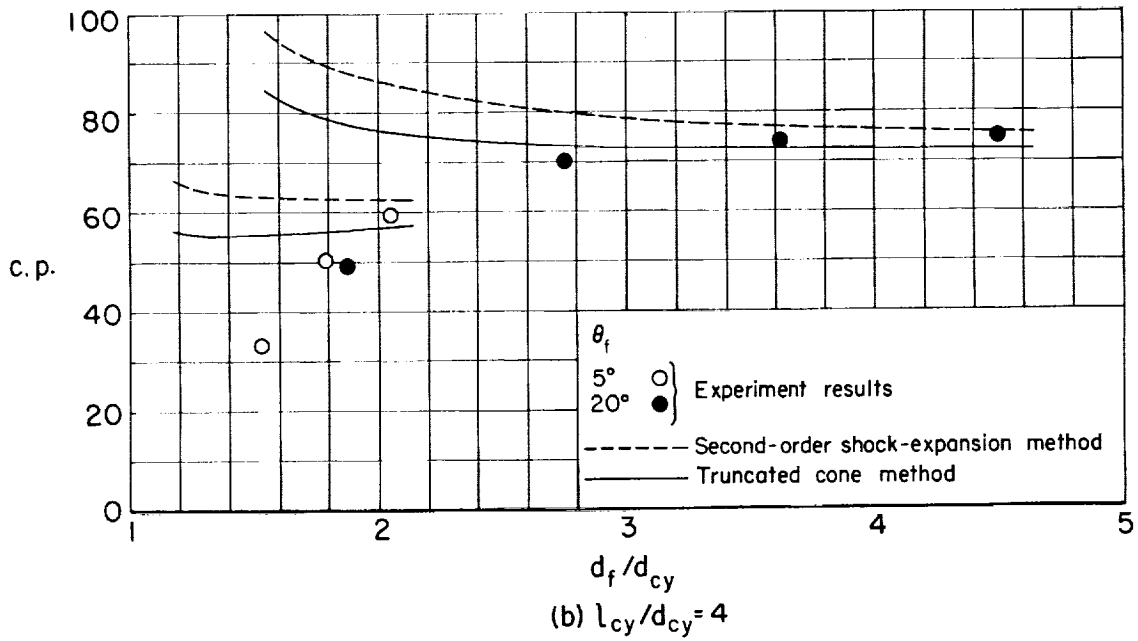
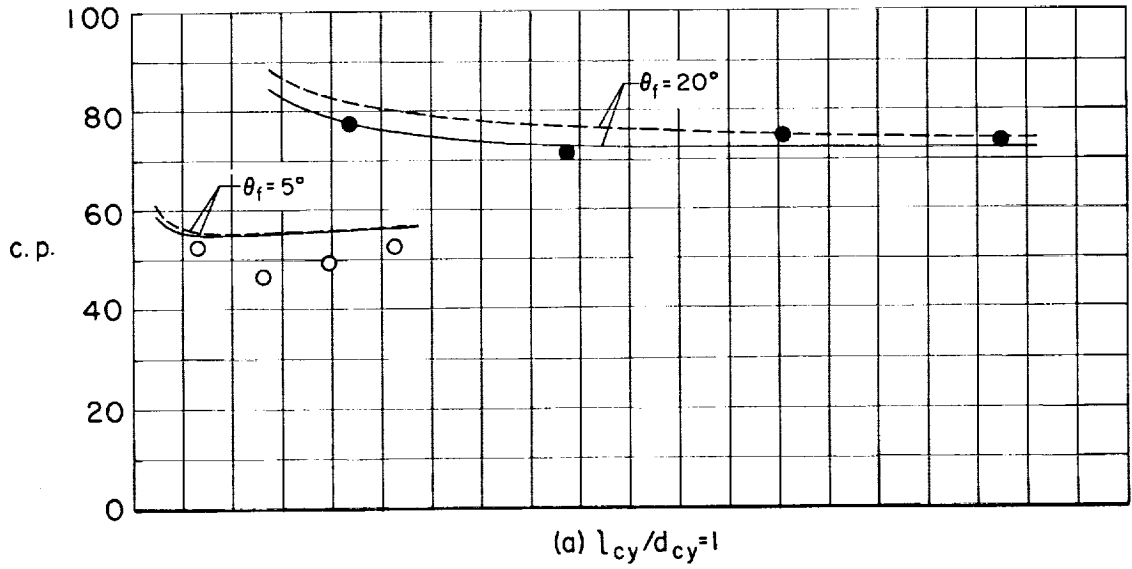


Figure 12.- Comparison of the flare center of pressure with that predicted by use of the second-order shock-expansion method,  $M = 2.81$ .



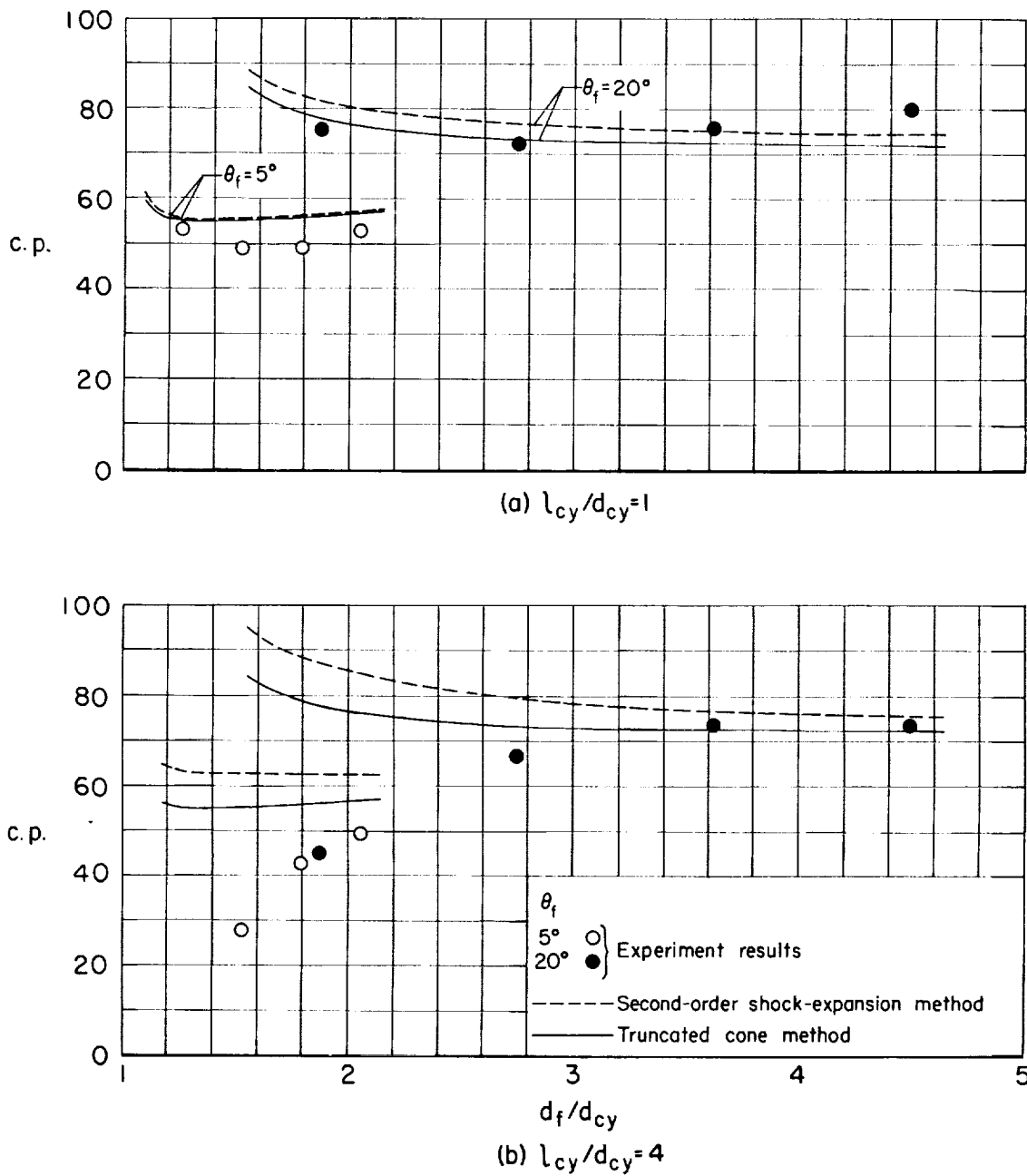


Figure 13.- Comparison of the flare center of pressure with that predicted by use of the second-order shock-expansion method,  $M = 4.04$ .

